Polymer Chemistry

Thermally Activated Delayed Fluorescence of Carbazole-Benzophenone Dendrimer with Bulky Substituents

Journal:	*Polymer Chemistry*
Manuscript ID	PY-ART-02-2022-000255
Article Type:	Paper
Date Submitted by the Author:	24-Feb-2022
Complete List of Authors:	Albrecht, Ken; Kyushu University; JST-PRESTO Hisamura, Eri; Kyushu University Furukori, Minori; National Institute of Advanced Industrial Science and Technology (AIST); Tokyo University of Science, Department of Pure and Applied Chemistry Nakayama, Yasuo; Tokyo University of Science, Department of Pure and Applied Chemistry; National Institute of Advanced Industrial Science and Technology (AIST) Hosokai, Takuya; National Institute of Advanced Industrial Science and Technology (AIST), Nakao, Kohei; Kyushu University Ikebe, Hiroki; Kyushu University Nakayama, Akira; The University of Tokyo, Department of Chemical System Engineering; Hokkaido University Catalysis Research Center,

SCHOLARONE™
Manuscripts

Please do not adjust margins

ARTICLE

Thermally Activated Delayed Fluorescence of Carbazole-Benzophenone Dendrimer with Bulky Substituents

Received 00th January 20xx,
Accepted 00th January 20xx

DOI: 10.1039/x0xx00000x

Ken Albrecht,*[a,b] Eri Hisamura,[a] Minori Furukori,[c,d] Yasuo Nakayama,[c,d] Takuya Hosokai,[d*] Kohei Nakao,[a] Hiroki Ikebe,[e] and Akira Nakayama[f]

Carbazole dendrimers with benzophenone core and bulky terminal substituents were synthesized, and thermally-activated delayed fluorescence (TADF) property was investigated. The adamantane (Ad) substituted dendrimer showed green TADF emission with PLQY of 40% in neat film. Tetrahenylphenyl (TPPh) substituted dendrimer showed blue emission with PLQY of 11 % in the neat film but did not show effective TADF. The dendrimer and dendron (fragment) phosphorescence measurement revealed that the TPPh substituted carbazole dendron has low triplet energy. This will reduce the TADF efficiency. Also a new deactivation path due to the large freedom in rotation of TPPh substituents leads to non-radiative deactivation and quenches the TADF emission. Simple terminal modification can minimize the intermolecular interaction and tune the on-off of the TADF, which gives insights for designing efficient TADF materials.

Introduction

Thermally activated delayed fluorescence (TADF)[1] material is a new class of emitting material that is gathering much attention for the use in organic light emitting diodes (OLED)[2] and much effort on understanding the mechanism[3] for improving the efficiency, such as from the view of photoluminescence quantum yield, [4] reverse intersystem crossing (RISC) rate,[5] narrow emission bandwidth,[6] and device stability[7] have been intensively studied. The key design concept of TADF materials is to reduce the energy between the singlet excited state and triplet excited state (ΔE_{ST}) by separating the hole and electron in the excited state but maintaining moderate recombination (fluorescence emission) rate. Additionally, for a high RISC rate (high spin-orbital coupling), the importance of engineering the energy level of the higher triplet states is pointed out.[3] Several donor-acceptor molecules with twisted π-conjugated bridge,[8] through-space interaction,[9] and bimolecular exciplex[10] state have been reported as efficient TADF material.

Emitting materials, including TADF, are often doped in a host material to inhibit concentration quenching and reduce roll-off (efficiency drop) at high current density in an OLED device. However, mixing materials make the process complicated. Controlling the doping rate at low concentrations is difficult in the vacuum deposition process, and phase separation is a potential threat in the solution process. Therefore, a single component emitting material (layer) that exhibits high photoluminescence quantum yield (PLQY) has been a research target. One approach to achieving high PLQY in the single-component (neat) film is introducing bulky substituents and reducing intermolecular interactions.[11] Another approach is to introduce the concept of AIE (aggregation induced emission) or AIEE (aggregation induced emission enhancement) materials[12], i.e., some molecular structures have high PLQY even in the solid state because the non-radiative deactivation path such as conical intersection is not accessible (or difficult to access) in solid-state. Based on these concepts, several TADF materials that achieve high PLQY in the neat film have been reported[13]. However, the first approach has intrinsically more chance to solve the roll-off problem, and the variety of bulky substituents will allow attaching additional properties such as self-host or charge-transporting property.[11] Overall, a new TADF material with high PLQY in neat film state is an important category that needs further development.

Solution-processed OLED has been a research target for a long time because of the essentially simple device fabrication process compared to the vacuum deposition process. Amorphous and smooth films are necessary for OLEDs, and sufficient solubility is required to prepare ink; therefore, usual low molecular weight materials are not suitable for the solution process. Solution-processable TADF materials have to also clear this requirement, and low to middle molecular weight materials with bulky structure,[11,14] polymers,[15] and dendrimers[16] have

[a] Institute of Materials Chemistry and Engineering, Kyushu University, 6-1, Kasuga Koen, Kasuga 816-8580, Japan
E-mail: albrecht@cm.kyushu-u.ac.jp
[b] JST-PRESTO, Honcho 4-1-8, Kawaguchi, Saitama 332-0012, Japan
[c] Department of Pure and Applied Chemistry, Graduate School of Science and Technology, Tokyo University of Science, 2641 Yamazaki, Noda, Chiba 278-8510, Japan
[d] National Metrology Institute of Japan (NMIJ), National Institute of Advanced Industrial Science and Technology (AIST), Tsukuba Central 5, 1-1-1 Higashi, Tsukuba, Ibaraki 305-8565, Japan
Email: t.hosokai@aist.go.jp
[e] Interdisciplinary Graduate School of Engineering Sciences, Kyushu University, 6-1 Kasuga-Koen Kasuga-shi Fukuoka 816-8580, Japan
[f] Department of Chemical System Engineering, Graduate School of Engineering, The University of Tokyo, Tokyo 113-8656, Japan
†Electronic Supplementary Information (ESI) available: Experimental section, synthesis, UV-vis spectra, PL spectra, PL life time data, and calculations. See DOI: 10.1039/x0xx00000x

Please do not adjust margins

been considered. Dendrimers[17] are branched polymers with exact molecular weight, and due to the high purity, structural designability, and high solubility, it has been employed as OLED materials. Especially, carbazole dendrimers have been extensively studied as TADF material because the unique polarized electronic structure[18] matches the design principle of TADF materials.[16] Some TADF dendrimers show high PLQY in a neat film state and can be utilized in multi-layer solution-processed devices[11b-d,15a,19]. However, most of the reports focus on changing the acceptor structure, and the effect of the terminal structure of carbazole dendron is not studied well. Previously we have demonstrated that the terminal structure strongly influences the TADF property of carbazole dendrimers by affecting the energy level and intermolecular intractions.[19a,d] Most literature only uses unsubstituted carbazole or 3,6-ditert-butyl group as terminal structure. The *tert*-buly substituted dendrimers show higher PLQY and device performance probably due to the bulkiness and oxidation stability. Herein we will report new carbazole-benzophenone dendrimers with a bulky terminal substituent that has never been employed for carbazole dendrimers and demonstrate that the terminal modification can strongly affect the TADF property.

Experimental section

The synthesis and structural characterization of the molecules are given in the ESI.† General experimental section, optical data, and calculation results are given in the ESI.†

Results and discussion

Synthesis

Three benzophenone core carbazole dendrimers with bulky substituents (adamantane = Ad, trityl = Tr, tetraphenylphenyl = TPPh) were designed and synthesized by using the copper catalyzed N-arylation reaction [20] as a key reaction (Scheme1,2). The Ad[21] and Tr[22] modified carbazoles were synthesized similarly to literature via Friedel-Crafts type aromatic electrophilic substitution reaction. The TPPh modified carbazole was synthesized via Diels-Alder reaction[23] of 3,6-diethynylcarbazole and tetraphenylcyclopentadienone. The G2 dendrons were synthesized similarly to the previously reported route, i.e., N-Arylation between modified carbazoles and silyl protected 3,6-diiodocarbazole (I2CzTBS) and following one-pot deprotection of silyl group.[16a] The TrCz had relatively low solubility, and TrG2on had extremely low solubility in common organic solvents. The formation of TrCzG2on was confirmed with MALDI-TOF-MS and ^{1}H NMR, but perfect purification and spectral characterization were difficult and the synthesis of the dendrimer was given up. Obtained two dendrons (Ad, TPPh) were reacted with 4,4'-diiodobenzophenone via N-arylation under microwave conditions to obtain corresponding carbazole-benzophenone dendrimers (AdG2B, and TPPhG2B). AdG2B and TPPhG2B were soluble in common organic solvents such as chloroform, THF, and toluene, indicating the capability as solution-processed OLED material. New compounds were characterized by ^{1}H, ^{13}C NMR, MALDI-TOF-MS, and elemental analysis.

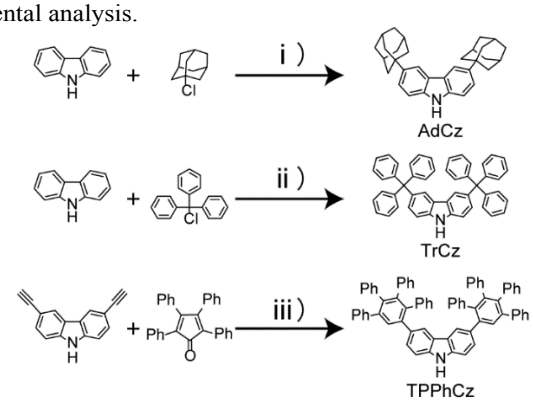

Scheme 1. The synthesis of carbazole derivatives. Reagents and Conditions i) $AlCl_3$, CH_2Cl_2, r.t., 24 h; ii) neat, 225 °C, 40 min.; iii) Xylene, reflux, 24 h.

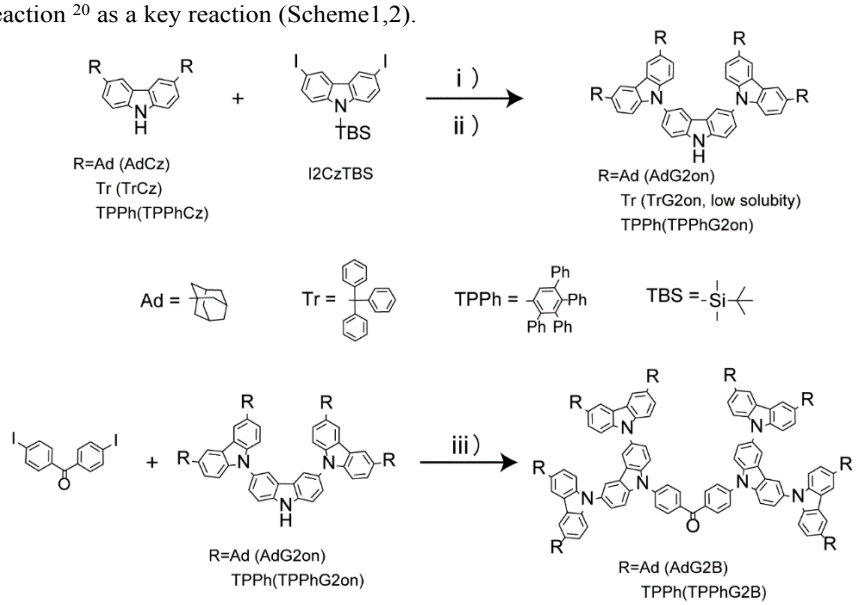

Scheme 2. Synthesis of carbazole G2 dendrons and benzophenone core dendrimers. Reagents and Conditions i) CuI, (±)-trans-1,2-Diaminocyclohexane, K_3PO_4, dioxane, 110 °C, 18 h; ii) TBAF, toluene, r.t., 0.75-2 h (one-pot reaction following the step i); iii) CuI, (±)-trans-1,2-Diaminocyclohexane, K_3PO_4, dioxane, 160 °C (microwave), 3 h;

This journal is © The Royal Society of Chemistry 20xx

Please do not adjust margins

Thermal property and film formation

A film of new dendrimers was fabricated by spin-coating the chloroform solution on a Si substrate, and the AFM images were obtained (Figs. S1,2). The images show that both dendrimer films have smooth surfaces in a wide (5 × 5 μm) range, but some irregular debris was also observed. The origin of the debris is not clear, but if severe crystallization or aggregation occurs, the images will have a much more rough surface over the whole image. Note that the images were obtained after 6 or 7 days of storage under ambient conditions supporting the long-term stability of the film. The roughness was calculated based on an enlarged image by excluding the region with debris. The RMS was ±0.5 nm (AdG2B), and ±0.6 nm (TPPhG2B), respectively. This indicates that the new dendrimers have the good film-forming property necessary for future device fabrication.

Thermogravimetric (TG) analysis of the dendrimers was performed to check the thermal stability (Fig. S3). The 5% weight loss temperature ($T_{d5\%}$) was 377 °C (AdG2B), and 576 °C (TPPhG2B), respectively. The DTG (differential TG) curve shows that decomposition of TPPhG2B starts from about 540 °C that is constant with previously reported carbazole based dendrimers.[16a,18i,24] On the other hand, the degradation of AdG2B started at about 210 °C followed by another degradation starting around 470 °C. TPPhG2B consists of an aromatic structure, but AdG2B contains a large amount of aliphatic (adamantane) components. The lower degradation of AdG2B starting at 210 °C and $T_{d5\%}$ at 377 °C can be attributed to partial decomposition of the adamantane group.[25] The aliphatic adamantane substitution decreases the decomposition temperature of the dendrimer, but still, both of the dendrimers have high thermal stability that is enough for future applications in an electronic device.

Photophysical property

The UV-vis absorption spectra of synthesized dendrimers in toluene and neat film state were recorded (Fig.1). Similar to previously reported carbazole-benzophenone dendrimers with other terminal substituents, the UV-vis spectra both in toluene and the neat film showed a weak absorption band at around 380 nm. This absorption is not existing in each fragment of the dendrimer (carbazole and benzophenone), and is attributed to the charge-transfer (CT) absorption from carbazole to benzophenone.

The PL spectra in solution and film state were observed (Fig.1). The PL spectra in toluene were quite similar for two dendrimers, and blue colored broad emission at 476 nm (AdG2B) and 474 nm (TPPhG2B) attributed to the emission from the CT excited state was observed. In the neat film, the PL shifted to 490 nm (AdG2B, green) and 470 nm (TPPhG2B, blue). The larger bathochromic shift of AdG2B is probably due to the change in the polarity of the media and intermolecular interactions (this point will be further discussed later). On the other hand, the slight hypsochromic shift of TPPhG2B indicates that the intermolecular interaction is minimum, and the emission center of the dendrimer is well shielded. Additionally, it probably reflects the low polarity environment that is provided with a large number of benzene rings similar to toluene. The shorter wavelength emission of TPPhG2B compared to AdG2B and excited CT character was also qualitatively reproduced by DFT calculation (Fig.S4, Table S1). The CT emission in the solution was also measured in various solvents with various polarities (Figs. S5-7, Tables S2,3). The large bathochromic shift when the polarity increased was observed, i.e., the emission at 476 nm (AdG2B) , and 474 nm (TPPhG2B) nm in toluene shifted to 629 nm (AdG2B) , and 614 nm (TPPhG2B) in DMSO. The emission peak energy had a linear relationship with the solvent polarity parameter (E_T^N),[26] indicating that the emission is from a single excited state. The large slope means that the dipole moment difference between the ground state and excited state is large. This is possibly attributed to the twisted intramolecular charge transfer (TICT) state.[19e,27] Overall, the new dendrimers show emission from CT excited state that most TADF materials show.

The photoluminescence quantum yield (PLQY) and PL decay were measured to determine the efficiency of TADF process (Table1, Fig.2). The PLQY of the toluene solution of AdG2B and TPPhG2B under nitrogen atmosphere was 66% and 43%, and decreased to 39% and 40% under air, respectively. The large drop in PLQY for AdG2B indicates the existence of a long lifetime component that can be assigned to TADF. The PLQY in neat film under nitrogen atmosphere was 40% (AdG2B) and 11% (TPPhG2B). This indicates that even the bulky substituent

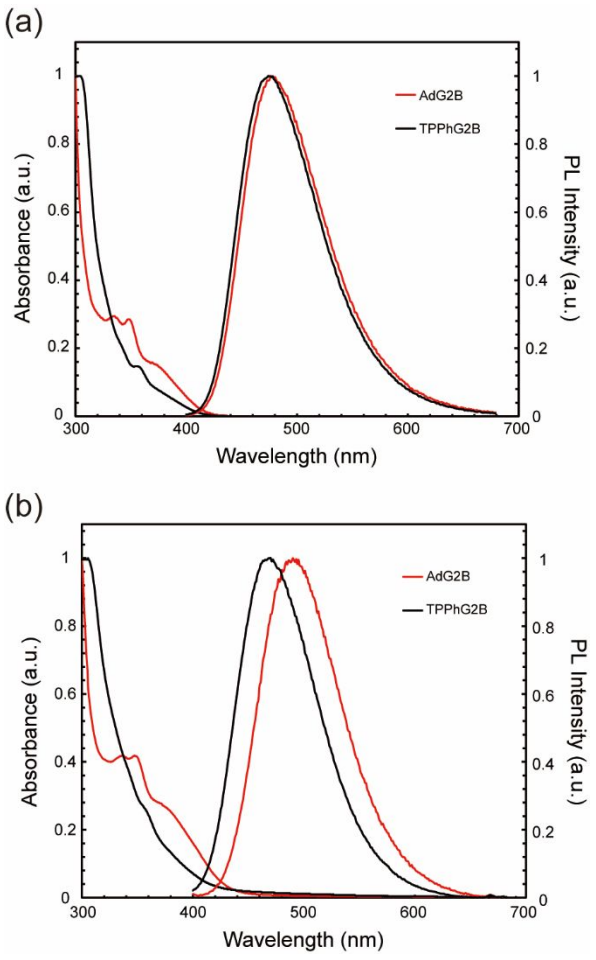

Figure 1 UV-vis spectra and PL spectra of dendrimers (a) toluene solution, and (b) neat film.

Table 1. Photophysical properties of AdG2B and TPPhG2B in toluene solution (sol) and neat films (film) (300 K).

	Φ_{PL} (air/degassed or in vacuum)	τ_F [ns] (air/degassed or in vacuum)	τ_{TADF} [ms] (air/degassed or in vacuum)	Φ_F	Φ_{TADF}	$k_F(10^7)$ [s^{-1}] a)	$k_{IC,T}(10^5)$ [s^{-1}] a)	$k_{ISC}(10^7)$ [s^{-1}] a)	$k_{RISC}(10^5)$ [s^{-1}] a)
AdG2B (solution)	39/66	6.3/7.0	-/5.1	39 c	27 d	5.6	1.1	8.7	2.2
AdG2B (film)	18/40	9.4/9.7 b	1.0/5.1	19 e	21 e	2.0	1.5	8.4	2.7
TPPhG2B (solution)	40/43	5.5/6.2	-/-	40 c	-	6.5	- f)	9.7	-
TPPhG2B (film)	11/11	4.5/4.5 b	-/-	11 c	-	2.4	- f)	28	-

a)Fluorescence decay rate (k_F), internal conversion decay rate from T_1 to S_0 ($K_{IC,T}$), intersystem crossing decay rate from S_1 to T_1 (k_{ISC}), and reverse intersystem crossing decay rate from T_1 to S_1 (k_{RISC}) are calculated from Φ_{PL}, Φ_F, Φ_{TADF}, τ_F , and τ_{TADF} according to ref 28, where non-radiative decay from S_1 to S_0 and ratiative decay from T_1 to S_0 are assumed to be zero. b) An average lifetime calculated by $\tau_{av}= \Sigma A_i\tau_i^2/ \Sigma A_i\tau_i$, where A_i is the pre-exponential for lifetime τ_i. c) Φ_{PL} in air. d) $\Phi_{TADF} = \Phi_{PL,\ degassed} - \Phi_F$. e) Calculated by integrated intensity ratio of prompt fluorescence and TADF in transient decay spectra (Fig. 2(c)) and Φ_{PL}. f) According to ref. 26, $k_{IC,T}$ cannot be determined due to the following definition, $k_{IC,T} = k_{TADF} - \Phi_F k_{RISC}$, where both k_{TADF} and k_{RISC} of TPPhG2B are zero.

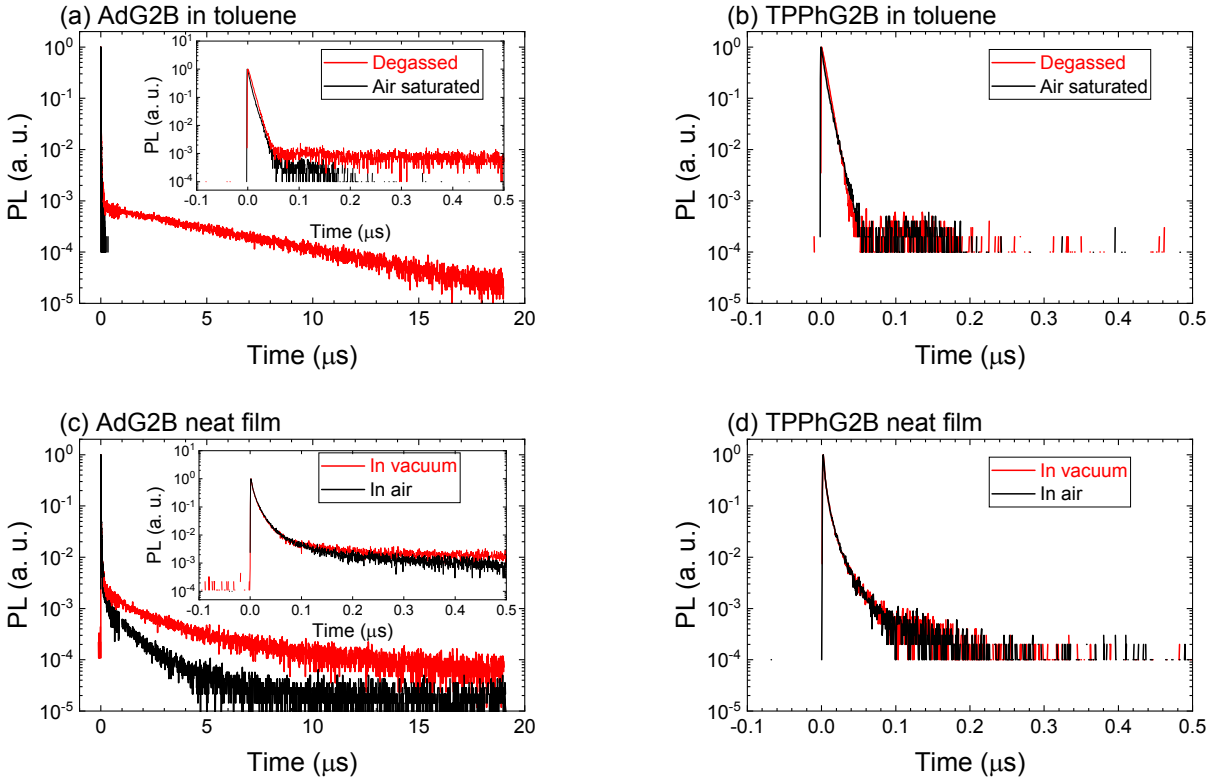

Figure 2. Transient decay spectra measured at 300 K; (a) AdG2B in toluene, (b) TPPhG2B in toluene, (c) AdG2B neat film, and (d) TPPhG2B neat film.

is attached to the periphery of the dendrimer, the PLQY drops in the neat film state compared to the toluene solution. Generally, concentration quenching takes place in the neat film compared to the dilute solution. However, the experiments that have been done in the next section have clarified that the drop in PLQY is not explained with simple concentration quenching. The PLQY drop is rather explained within change of the excited state dynamics because the polarity of the medium changes, and the motion of the dendrimer is restricted in the film state. The PL lifetime of the neat film of AdG2B clearly shows the existence of ns order short lifetime component and μs order long lifetime component. The PL spectra of the short and long lifetime components are almost identical and are attributed to the prompt fluorescence and TADF. The estimated k_{RISC} rate constant was the order of 10^{-5} s^{-1}, which is similar to other carbazole-benzophenone dendrimers.[19d,e] On the other hand, the PL decay profile of TPPhG2B showed almost only the short lifetime component. Interestingly these data indicate that the terminal modification of the dendrimer switches the on and off of the TADF.

The effectiveness of the bulky substituent on inhibiting unsuitable intramolecular interaction was determined by

This journal is © The Royal Society of Chemistry 20xx

measuring the PL, PLQY, and PL decay of dendrimer doped PMMA films. A PMMA film containing dendrimers in 10, 30,50, 80, and 100wt% (neat) was prepared by spin-costing the chloroform solution, and PL spectra were measured (Fig.S11). The PL spectra showed a slight blue shift compared to the neat film prepared from the toluene solution. For both AdG2B and TPPhG2B, the PL spectra showed only minimum change while increasing the concentration. This behavior is in clear contrast with the previous experiment using carbazole benzophenone dendrimer with terminal H, Me, MeO, and *t*-Bu group, i.e., relatively large red-shift took place with these substituents.[19d] During the concentration increase, the PLQY was also maintained, and the PL decay behavior was also identical (Figs. S12,13). The comparison of PL spectra in toluene solution and neat film (Fig.1) is complex because it reflects changes in the environment (polarity), molecular motion, and intermolecular interaction. The PMMA doped film experiment revealed that carbazole-benzophenone dendrimer with Ad and TPPh groups are almost perfectly isolated even in neat film. The PL is insensitive to the host environment because the bulky substituents dominate the polarity and inhibit intermolecular interactions around the luminescent core.

To further investigate the influence of terminal structure on the TADF efficiency, the ^{1}CT, ^{3}CT, and ^{3}LE energy levels were determined. The ^{1}CT and ^{3}CT energy level was determined from the onset of the fluorescence and phosphorescence spectra of the frozen toluene solution and neat film at 77 K (Table2, Figs.S8, 9). The ^{3}LE energy level of the donor unit (carbazole dendrons) was also determined from the onset of the phosphorescence spectra of the toluene solution and neat film at 77 K (Figs.S8, 9). The phosphorescence spectra of AdG2B and AdG2on had small time dependence, but TPPhG2B and TPPhG2on showed complicated time dependence. This is probably reflecting the unevenness of the molecular conformations (larger distribution of conformations) due to the rotation of benzene rings of the TPPh group and the complex excited-state dynamics. For figuring out the actual reason, some time-resolved absorption spectroscopy is necessary. The ΔE_{ST} value of AdG2B was smaller than TPPhG2B in the solution and neat film. Smaller ΔE_{ST} will usually lead to a larger RISC (reverse intersystem crossing) process, i.e., TADF expression in AdG2B can be explained in part. However, TPPhG2B also has a relatively small ΔE_{ST} for TADF expression (0.16 eV in toluene solution and 0.09 eV in neat film). The difference in ΔE_{ST} was also quallitatively reproduced with DFT calculation of S_1 excited state (TableS1). The calculated absolute value was larger than the observed value, partly because the polarizable continuum solvation model is not sufficient for including environmental effects for long-range CT states, which was similar to the previous report.[19d] The position between the ^{3}CT and ^{3}LE is often discussed to explain the true efficiency of the RISC process. In principle, the RISC process between the ^{3}CT and ^{1}CT state is forbidden and the spin-flip process through the hyperfine coupling is slow. The mediation of ^{3}LE has an important role in increasing SOC (spin-orbital coupling) for the efficient RISC process, and this effect will be larger when the gap between ^{3}CT and ^{3}LE decreases. The S_1, ^{3}CT, and ^{3}LE levels of AdCz are distributed in a narrow range suitable for the efficient TADF (RISC) process (Fig.S10). On the otherhand, the ^{3}LE state of TPPhG2B lies under the ^{3}CT state and results in larger activation energy for the TADF (RISC) process (Fig.S10). Furthermore, the time dependence of the phosphorescence spectra of TPPh derivatives indicates the complex dynamics, which may lead to deactivation paths. The phosphorescence of TPPhG2on was weak indicating the existence of a deactivation path from ^{3}LE state (Fig.S9). The broad phosphorescence spectra of TPPhG2B suggest that the phosphorescence is dominated with emission from ^{3}CT even the ^{3}LE state lies under ^{3}CT, and this also supports that ^{3}LE state undergoes a non-radiative deactivation. Through measuring the energy levels of new dendrimers, the on-off of TADF upon terminal modification was explained as following, i.e., AdG2B has energy level alignment that is suitable for TADF, but energy level alignment of TPPhG2B is worse and larger deactivation path from the ^{3}LE state exists.

Table 2. Energy levels of carbazole dendrimers.

	HOMO (eV) [a]	LUMO (eV) [b]	S_1 (eV) [c]	^{3}CT (eV) [c]	ΔEs-t (eV) [c]	^{3}LE (eV) [d]
AdG2B (solution)	–	-	2.96	2.89	0.07	3.02
AdG2B (film)	5.68	2.80	2.86	2.83	0.03	2.88
TPPhG2B (solution)	–	–	3.04	2.88	0.16	2.87
TPPhG2B (film)	5.71	2.77	2.96	2.87	0.09	2.75

[a] Determined by photoelectron spectroscopy in air of the film; [b] Estimated from the HOMO level and absorption edge; [c] Estimated from the onset of the fluorescence and phosphorescence spectra; [d] Estimated from the onset of the phosphorescence spectra of carbazole dendrons;

Conclusions

New benzophenone core carbazole dendrimers with bulky substituents (adamantane, tetraphenylphenyl) that have been for the first time introduced to carbazole dendrimer were synthesized and photophysical properties were investigated. The bulky substituents were not sufficient to perfectly suppress concentration quenching, but the neat film of AdG2B showed green emission with PLQY of 40%, and TPPhG2B showed greenish-blue emission with PLQY of 11% in neat film. The PL decay measurements revealed that AdG2B shows efficient TADF, but TPPh does not show TADF. The reason was attributed to the larger ΔE_{ST}, larger ^{3}CT-^{3}LE (ΔT-T) energy gap, and the existence of other deactivation paths related to the rotation of benzene rings. New carbazole units with bulky substituents will offer new options for donor design in TADF materials and archives nearly perfect isolation of the molecules. OLED device fabrication with the present dendrimers has not been performed due to the relatively low PLQY. Further optimization of the dendrimer structure with bulky terminal groups, such as acceptor and linkage design, will lead to efficient solution-processable TADF dendrimers with minimal concentration quenching and efficient OLED device performance.

Author Contributions

The manuscript was written through the contributions of all authors. All authors have approved the final version of the manuscript. K. A. wrote the main body of the manuscript with assistance from all authors. K. A. designed the research. Synthesis, characterization, and majority of measurements were performed by E. H. with the help of H. I. and K. N. under the supervision of K. A. Time resolved fluorescence and some photophysical measurements were performed by M. F. under the supervision of T. H and Y. N. Data processing was performed by K. A., T. H. and A. N. Also, A N. performed and reported the DFT calculations. Thermal analysis was performed by K. N and H. I. The AFM images were obtained by Y. N. The funding for this work was obtained jointly by K. A, Y. N. and T. H.

Conflicts of interest

The authors declare no competing financial interest.

Acknowledgments

This work was supported, in part, by JSPS KAKENHI Grant No. JP18H03902, JP20H02801, JP21H05399 and JP21H05405. JST PRESTO Grant Number JPMJPR18T2, Tobe Maki foundation, and the Futaba Foundation. Leading Initiative for Excellent Young Researchers, microstructural characterization platform as a program of “Nanotechnology Platform” Grant Number JPMXP09A19AT0001, and Cooperative Research Program of "Network Joint Research Center for Materials and Devices", Grant Number 20201309 of the Ministry of Education, Culture, Sports, Science and Technology (MEXT). Part of the calculations was performed on supercomputers at RCCS (Okazaki), RIIT (Kyushu Univ.), and the Center for Computational Materials Science, Institute for Materials Research (Tohoku University, Proposal No. 202012-SCKXX-0012).

Notes and references

1 (a) C. A. Parker and C. G. Hatchard, *Trans. Faraday Soc.*, 1961, **57**, 1894–1904; (b) A. Maciejewski, M. Szymanski and R. P. Steer, *J. Phys. Chem.*, 1986, **90**, 6314–6318; (c) M. N. Berberan-Santos and J. M. M. Garcia, *J. Am. Chem. Soc.*, 1996, **118**, 9391–9394.

2 (a) A. Endo, M. Ogasawara, A. Takahashi, D. Yokoyama, Y. Kato and C. Adachi, *Adv. Mater.*, 2009, **21**, 4802; (b) J. C. Deaton, S. C. Switalski, D. Y. Kondakov, R. H. Young, T. D. Pawlik, D. J. Giesen, S. B. Harkins, A. J. M. Miller, S. F. Mickenberg and J. C. Peters, *J. Am. Chem. Soc.*, 2010, **132**, 9499–9508; (c) F. B. Dias, K. N. Bourdakos, V. Jankus, K. C. Moss, K. T. Kamtekar, V. Bhalla, J. Santos, M. R. Bryce and A. P. Monkman, *Adv. Mater.*, 2013, **25**, 3707–3714.

3 (a) F. B. Dias, K. N. Bourdakos , V. Jankus, K. C. Moss, K. T. Kamtekar, V. Bhalla, J. Santos, M. R. Bryce and Andrew P. Monkma, *Adv. Mater.* 2013, **25**, 3707; (b) M. K. Etherington, J. Gibson, H. F. Higginbotham, T. J. Penfold and A. P. Monkman, *Nat. Commun.*, 2016, *7*, 13680; (c) P. K. Samanta, D. Kim, V. Coropceanu and J. Brédas, *J. Am. Chem. Soc.*, 2017, **139**, 4042. (d) T. Hosokai, H. Matsuzaki, H. Nakanotani, K. Tokumaru, T. Tsutsui, A. Furube, K. Nasu, H. Nomura, M. Yahiro and C. Adachi, *Sci. Adv.*, 2017, **3**, e1603282; (e) T. J. Penfold, E. Gindensperger, C. Daniel and C. M. Marian, *Chem. Rev.*, 2018, **118**, 6975. (f) H. Noda, X. Chen, H. Nakanotani, T. Hosokai, M. Miyajima, N. Notsuka, J. Brédas and C. Adachi, *Nat. Mater.*, 2019, **18**, 1084–1090.

4 H. Uoyama, K. Goushi, K. Shizu, H. Nomura and C. Adachi, *Nature*, 2012, **492**, 234.

5 (a) L.-S. Cui, A. J. Gillett, S.-F. Zhang, H. Ye, Y. Liu, X.-K. Chen, Z.-S. Lin, E. W. Evans, W. K. Myers, T. K. Ronson, H. Nakanotani, S. Reineke, J.-L. Bredas, C. Adachi and R. H. Friend, *Nat. Photon.*, 2020, **14**, 636–642; (b) Y. Wada, H. Nakagawa, S. Matsumoto, Y. Wakisaka and H. Kaji, *Nat. Photon.*, 2020, **14**, 643–649.

6 (a) T. Hatakeyama, K. Shiren, K. Nakajima, S. Nomura, S. Nakatsuka, K. Kinoshita, J. Ni, Y. Ono and T. Ikuta, *Adv. Mater.*, 2016, **28**, 2777–2781; (b) Y. Kondo, K. Yoshiura, S. Kitera, H. Nishi, S. Oda, H. Gotoh, Y. Sasada, M. Yanai and T. Hatakeyama, *Nat. Photon.*, 2019, **13**, 678–682.

7 (a) H. Nakanotani, T. Higuchi, T. Furukawa, K. Masui, K. Morimoto, M. Numata, H. Tanaka, Y. Sagara, T. Yasuda and C. Adachi, *Nat. Commun.*, 2014, **5**, 4016; (b) S. O. Jeon, K. H. Lee, J. S. Kim, S.-G. Ihn, Y. S. Chung, J. W. Kim, H. Lee, S. Kim, H. Choi and J. Y. Lee, *Nat. Photon.*, 2021, **15**, 208–215.

8 (a) H. Tanaka, K. Shizu, H. Nakanotani and C. Adachi, *Chem. Mater.*, 2013, **25**, 3766–3771; (b) I. Park, H. Komiyama and T. Yasuda, *Chem. Sci.*, 2016, **8**, 953–960; (c) P. Data, P. Pander, M. Okazaki, Y. Takeda, S. Minakata and A. P. Monkman, *Angew. Chem. Int. Ed.*, 2016, **55**, 5739–5744.

9 (a) K. Kawasumi, T. Wu, T. Zhu, H. Chae, T. Voorhis, M. A. Baldo and T. M. Swager, *J. Am. Chem. Soc.*, 2015, **137**, 11908–11911; (b) Y. Wang, C. Huang, H. Ye, C. Zhong, A. Khan, S. Yang, M. Fung, Z. Jiang, C. Adachi and L. Liao, *Adv. Opt. Mater.*, 2020, **8**, 1901150. (c) Y. Wada, H. Nakagawa, S. Matsumoto, Y. Wakisaka and H. Kaji, *Nat. Photon.*, 2020, **14**, 643–649.

10 (a) M. Sarma and K.-T. Wong, *ACS Appl. Mater. Interfaces*, 2018, **10**, 19279–19304; (b) K. Goushi, K. Yoshida, K. Sato and C. Adachi, *Nat. Photon.*, 2012, **6**, 253–258; (c) M. Colella, P. Pander, D. de S. Pereira and A. P. Monkman, *ACS Appl. Mater. Interfaces*, 2018, **10**, 40001–40007.

11 (a) X. Ban, W. Jiang, T. Lu, X. Jing, Q. Tang, S. Huang, K. Sun, B. Huang, B. Lin and Y. Sun, *J. Mater. Chem. C*, 2016, **4**, 8810–8816; (b) X. Ban, A. Zhu, T. Zhang, Z. Tong, W. Jiang and Y. Sun, *ACS Appl. Mater. Interfaces*, 2017, **9**, 21900–21908; (c) D. Liu, W. Tian, Y. Feng, X. Zhang, X. Ban, W. Jiang and Y. Sun, *ACS Appl. Mater. Interfaces*, 2019, **11**, 16737–16748; (d) X. Ban, Y. Liu, J. Pan, F. Chen, A. Zhu, W. Jiang, Y. Sun and Y. Dong, *ACS Appl. Mater. Interfaces*, 2020, **12**, 1190–1200; (e) Z. Ma, Y. Wan, W. Dong, Z. Si, Q. Duan and S. Shao, *Chin. Chem. Lett.*, 2020, **32**, 703–707.

12 (a) G. R. Suman, M. Pandey and A. S. J. Chakravarthy, *Mater. Chem. Front.*, 2020, **5**, 1541–1584; (b) S. Suzuki, S. Sasaki, A. S. Sairi, R. Iwai, B. Z. Tang and G. Konishi, *Angew. Chem. Int. Ed.*, 2020, **59**, 9856–9867.

13 (a) R. Furue, T. Nishimoto, I. Park, J. Lee and T. Yasuda, *Angew. Chem. Int. Ed.*, 2016, **55**, 7171–7175; (b) H. J. Kim, S. K. Kim, M. Godumala, J. Yoon, C. Y. Kim, J.-E. Jeong, H. Y. Woo, J. H. Kwon, M. J. Cho and D. H. Choi, *Chem. Commun.*, 2019, **55**, 9475–9478; (c) D. Liu, J. Y. Wei, W. W. Tian, W. Jiang, Y. M. Sun, Z. Zhao and B. Z. Tang, *Chem. Sci.*, 2020, **11**, 7194–7203; (d) Z. Cai, H. Chen, J. Guo, Z. Zhao and B. Z. Tang, *Front. Chem.*, 2020, **8**, 193; (e) B. Huang, Y. Ji, Z. Li, N. Zhou, W. Jiang, Y. Feng, B. Lin and Y. Sun, *J. Lumin.*, 2017, **187**, 414–420.

14 (a) Y. Cho, K. Yook and J. Lee, *Adv. Mater.*, 2014, **26**, 6642–6646; (b) Y. Wada, K. Shizu, S. Kubo, K. Suzuki, H. Tanaka, C.

 This journal is © The Royal Society of Chemistry 20xx

Adachi and H. Kaji, *Appl. Phys. Lett.*, 2015, **107**, 183303; (c) D. Di, A. S. Romanov, L. Yang, J. M. Richter, J. P. H. Rivett, S. Jones, T. H. Thomas, M. A. Jalebi, R. H. Friend, M. Linnolahti, M. Bochmann and D. Credgington, *Science*, 2017, **356**, 159–163.

15 (a) A. E. Nikolaenko, M. Cass, F. Bourcet, D. Mohamad and M. Roberts, *Adv. Mater.*, 2015, **27**, 7236–7240; (b) J. Luo, G. Xie, S. Gong, T. Chen and C. Yang, *Chem. Commun.*, 2016, **52**, 2292–2295; (c) Z. Ren, R. S. Nobuyasu, F. B. Dias, A. P. Monkman, S. Yan and M. R. Bryce, *Macromolecules*, 2016, **49**, 5452–5460; (d) S. Lee, T. Yasuda, H. Komiyama, J. Lee, C. Adachi, *Adv. Mater.* **2016**, *28*, 4019; (e) P. Khammultri, W. Kitisriworaphan, P. Chasing, S. Namuangruk, T. Sudyoadsuk and V. Promarak, *Polym. Chem.*, 2021, **12**, 1030–1039. (f) T. Jiang, Y. Liu, Z. Ren and S. Yan, *Polym. Chem.*, 2020, **11**, 1555–1571.

16 (a) K. Albrecht, K. Matsuoka, K. Fujita and K. Yamamoto, *Angew. Chem. Int. Ed.*, 2015, **54**, 5677–5682; (b) B. Huang, X. Ban, K. Sun, Z. Ma, Y. Mei, W. Jiang, B. Lin and Y. Sun, *Dyes Pigm.*, 2016, **133**, 380; (c) J. Li, X. Liao, H. Xu, L. Li, J. Zhang, H. Wang and B. Xu, *Dyes Pigm.*, 2017, **140**, 79; (d) Y. Li, G. Xie, S. Gong, K. Wu and C. Yang, *Chem. Sci.*, 2016, **7**, 5441; (e) J. Luo, S. Gong, Y. Gu, T. Chen, Y. Li, C. Zhong, G. Xie and C. Yang, *J. Mater. Chem. C*, 2016, **4**, 2442; (f) S. Gong, J. Luo, Z. Wang, Y. Li, T. Chen, G. Xie and C. Yang, *Dyes Pigm.*, 2017, **139**, 593; (g) K. Sun, Y. Sun, T. Huang, J. Luo, W. Jiang and Y. Sun, *Org. Electron.*, 2017, **42**, 123; (h) X. Ban, W. Jiang, T. Lu, X. Jing, Q. Tang, S. Huang, K. Sun, B. Huang, B. Lin and Y. Sun, *J Mater. Chem. C*, 2016, **4**, 8810; (i) X. Wang, J. Hu, J. Lv, Q. Yang, H. Tian, S. Shao, L. Wang, X. Jing, F. Wang, *Angew. Chem. Int. Ed.* **2021**, *60*, 16585.

17 (a) D. A. Tomalia, H. Baker, J. Dewald, M. Hall, G. Kallos, S. Martin, J. Roeck, J. Ryder and P. Smith, *Polym. J.*, 1985, **17**, 117–132; (b) D. Astruc, E. Boisselier, C. Ornelas, *Chem. Rev.* **2010**, *110*, 1857.

18 (a) K. Albrecht and K. Yamamoto, *J. Am. Chem. Soc.*, 2009, **131**, 2244–2251; (b) N. D. McClenaghan, R. Passalacqua, F. Loiseau, S. Campagna, B. Verheyde, A. Hameurlaine and W. Dehaen, *J. Am. Chem. Soc.*, 2003, **125**, 5356; (c) Y. Xing, H. Lin, F. Wang a nd P. Lu, *Sens. Actuators B Chem.*. 2006, **114**, 28; (d) K. A. Knights, S. G. Stevenson, C. P. Shipley, S.-C. Lo, S. Olsen, R. E. Harding, S. Gambino, P. L. Burn and I. D. W. Samuel, *J. Mater. Chem.*, 2008, **18**, 2121; (e)T. Xu, R. Lu, M. Jin, X. Qiu, P. Xue, C. Bao and Y. Zhao, *Tetrahedron Lett.* 2005, **46**, 6883; (f) A. Kimoto, J. Cho, M. Higuchi, K. Yamamoto, *Macromolecules*, 2004, **37**, 5531; (g) S. Gambino, S. G. Stevenson, K. a. Knights, P. L. Burn and I. D. W. Samuel, *Adv. Funct. Mater.*, 2009, **19**, 317; (h) K. Mutkins, S. S. Y. Chen, A. Pivrikas, M. Aljada, P. L. Burn, P. Meredith and B. J. Powell, *Polym. Chem.*, 2013, **4**, 916; (i) K. Albrecht, Y. Kasai, A. Kimoto and K. Yamamoto, *Macromolecules*, 2008, **41**, 3793–3800.

19(a) K. Albrecht, K. Matsuoka, D. Yokoyama, Y. Sakai, A. Nakayama, K. Fujita and K. Yamamoto, *Chem. Commun.*, 2017, **53**, 2439–2442; (b) K. Albrecht, K. Matsuoka, K. Fujita and K. Yamamoto, *Mater. Chem. Front.*, 2018, **2**, 1097–1103; (c) A. C, B. Luszczynska, M. Z. Szymanski, J. Ulanski, K. Albrecht and K. Yamamoto, *Org. Electron.*, 2019, **74**, 218–227; (d) K. Matsuoka, K. Albrecht, A. Nakayama, K. Yamamoto and K. Fujita, *ACS Appl. Mater. Interfaces*, 2018, **10**, 33343–33352; (e) K. Matsuoka, K. Albrecht, K. Yamamoto and K. Fujita, *Sci. Rep.*, 2017, **7**, 41780.

20 A. Klapars, J. C. Antilla, X. Huang and S. L. Buchwald, *J. Am. Chem. Soc.*, 2001, **123**, 7727–7729.

21 *JP Pat.*, JP 2013-108015, 2013.

22 S. Matsumura, A. R. Hlil, N. Du, C. Lepiller, J. Gaudet, D. Guay, Z. Shi, S. Holdcroft and A. S. Hay, *J. Polym. Sci. A Polym. Chem.*, 2008, **46**, 3860–3868.

23 Q. Xiang, X. Sun, G. Zhu, H. Sun, Y. Wan, Z. Si and Q. Duan, *Eur J Inorg Chem*, 2012, **2012**, 4012–4019.

24 K. Albrecht, R. Pernites, M. Felipe, R. C. Advincula and K. Yamamoto, *Macromolecules*, 2012, **45**, 1288–1295.

25 a) T. Ishizone, H. Tajima, S. Matsuoka and S. Nakahama, *Tetrahedron Lett*, 2001, **42**, 8645–8647. b) T. Ishizone, *Kobunshi*, 2004, **53**, 342-347. c) L. J. Mathias and G. L. Tullos, *Polymer*, 1996, **37**, 3771–3774.

26 C. Reichardt, *Chem Rev*, 1994, **94**, 2319–2358.

27 F. Loiseau, S. Campagna, A. Hameurlaine and W. Dehaen, *J. Am. Chem. Soc.*, 2005, **127**, 11352–11363.

28 K. Masui, H. Nakanotani, C. Adachi, *Org. Electon.*, 2013, **14**, 2721.